3C7 Structure Research Lab (Stress Analysis) Report

Louis Z (lz406) Fitzwilliam College

online session on Wed. 21st Oct 2020

SUMMARY

3C7 lab used 3 experimental techniques (***A.*** photo-elasticity ***B.*** Strain gauges ***C.*** Digital Image Correlation) to show stress concentrations distribution induced by ***A.*** a symmetrically located circular hole, ***B.***an asymmetrically hole in a thin aluminium plate loaded in uniaxial tension, the measured results is then compared with solutions from 3 analytical methods.
Subsequently, a qualitative overall picture of the strain distribution is given by the visualisation of a deformed elastomer plate under the same loading.

INTRODUCTION

Whenever there are irregularities in the geometry of a structural component (e.g. holes, grooves, notches and fillets), stresses in such locations (geometric discontinuities) are significantly greater than the surrounding regions.
For both ductile and brittle material, plastic deformation or failure typically first happen at a stress concentration. However, for repeated low-level loading where elasticity theory is applicable, fatigue cracks always initiate slowly develop and at a stress concentration which eventually leading to structure failure.
The 3C7 lab is therefore to investigate the stress distributions in the vicinity of a circular hole in a uniaxially loaded thin plate, and so to give an understanding of the great practical importance geometric discontinuities have on the stress concentrations.

∘Aloha Airlines Flight 243 (1988) suffered an explosive decompression and fuselage failure resulted by multiple site fatigue cracking of the skin adjacent to rivet holes along a lap joint rivet row. The knife edge concentrated stresses around rivet holes resulted in the lap joint disbanding, and sadly 1 fatality in the incident.

EXPERIMENTAL & ANALYTICAL RESULTS

Measured stains through strain-gauges:

Symmetric Plate			Asymmetric Plate		
Gauge No	$\varepsilon(2kN)$	$\varepsilon(4kN)$	*Gauge No*	$\varepsilon(2kN)$	$\varepsilon(4kN)$
1	0.000467	0.000475	1	0.000158	0.000350
2	-0.000175	-0.000175	2	0.000242	0.000525
3	0.000550	0.000559	3	-0.000033	-0.000083
4	-0.000175	-0.000175	4	0.000525	0.001085
5	0.000609	0.000617	5	0.000108	0.000258
6	0.000801	0.000809	6	-0.000175	-0.000342
7	-0.000208	-0.000208	7	0.000467	0.000968
8	0.000550	0.000567	8	-0.000017	-0.000042
9	0.000475	0.000475	9	0.000175	0.000383
10	0.000358	0.000358	10	-0.000042	-0.000083
11	-0.000300	-0.000308	11	0.000150	0.000325
12	0.000317	0.000317	12	0.000125	0.000275

Displacements observed in the elastomer plate (with symmetrically located hole):

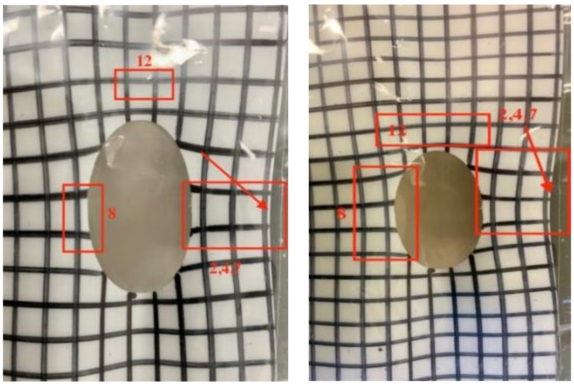

It is observed in the deformed elastomer that: ***A.***in region corresponds to strain gauges 2,4,7 (is marked in the pictures using symmetry), the plate is “compressed” in horizontal direction. i.e.$\varepsilon_2, \varepsilon_4, \varepsilon_7$<0. ***B.*** in region corresponds to strain gauge12, the plate is “stretched” in horizontal direction. i.e. ε_{12}>0. ***C.*** in region corresponds to strain gauge 8, the plate is “stretched” vertically, i.e. ε_8>0.
As shown, measured strains qualitatively agree with displacements observed in the elastomer plate. (although due to its deformation in 3D, the elastomer plate is not in a state of plane stress as the metal plate)

Calculated stresses on Symmetric Plate:

Symmetric Plate (2kN)					
Gauge No	$\sigma_{xx}/10^7$ Pa	Gauge No	$\sigma_{yy}/10^5 Pa$	Gauge No	$\sigma_{xy}/10^7$Pa
1	3.269	2	9.0338	10	-1.424
3	3.880	4	24.33		
5	4.343	7	42.68		
6	5.748	11	-112.5		
8	3.850	12	221.9		
9	2.954				

Symmetric Plate (4kN)					
Gauge No	$\sigma_{xx}/10^7 Pa$	Gauge No	$\sigma_{yy}/10^5 Pa$	Gauge No	$\sigma_{xy}/10^7 Pa$
1	3.325	2	11.37	10	-1.45
3	3.951	4	26.402		
5	4.406	7	44.75		
6	5.811	11	-120.385		
8	3.969	12	221.9		
9	2.928				

Analytical solution given by Howland derivation:

Symmetric Plate			
σ_{xx} at point $A/10^7$ Pa		σ_{yy} at point $B/10^7 Pa$	
2kN	4kN	2kN	4kN
3.953	7.906	-1.482	-2.965

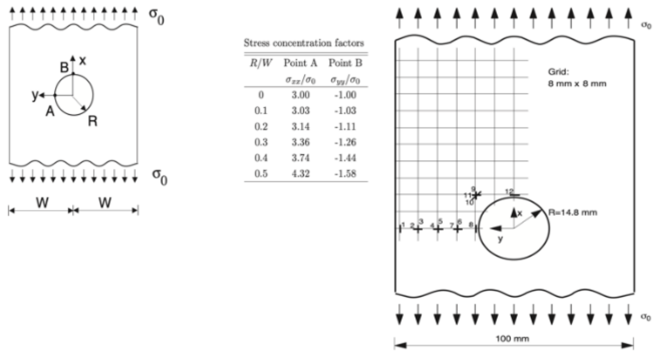

R/W≈0.3 for Howland derivation, analytical solution for $\sigma_{xx,point\ A}$ roughly agree with measured stress $\sigma_{xx,Gauge\ 8}$, but there is a large discrepancy in magnitude under 4kN loading condition.
Analytical solution for $\sigma_{yy,point\ B}$ suggests a compressive stress immediate on the top edge of the symmetric hole, which can be visualised by the “compressive” strain on the same area of the deformed elastomer plate. Point B is unlikely on the same location as strain-gauge 12, with gauge 12 assumed to be located further up in the +ve x-direction.

Calculated stresses on Asymmetric Plate:

Asymmetric Plate (2kN)					
Gauge No	$\sigma_{xx}/10^7 Pa$	Gauge No	$\sigma_{yy}/10^6 Pa$	Gauge No	$\sigma_{xy}/10^6 Pa$
1	1.106	3	3.681	5	3.658
2	1.815	6	-11.900		
4	3.675	8	3.201		
7	3.269	10	0.589		
9	1.331				
11	1.069				
12	0.875				

Asymmetric Plate (4kN)					
Gauge No	$\sigma_{xx}/10^7 Pa$	Gauge No	$\sigma_{yy}/10^6 Pa$	Gauge No	$\sigma_{xy}/10^6 Pa$
1	2.450	3	7.090	5	6.026
2	3.909	6	-23.800		
4	7.595	8	6.629		
7	6.776	10	1.905		
9	2.900				
11	2.338				
12	1.925				

Analytical solution given by Mindlin derivation:

Asymmetric Plate				
σ_{xx} at point $A/10^7 Pa$			σ_{xx}at point $B/10^6 Pa$	
2kN	4kN		2kN	4kN
4.635	9.271		6.941	13.882

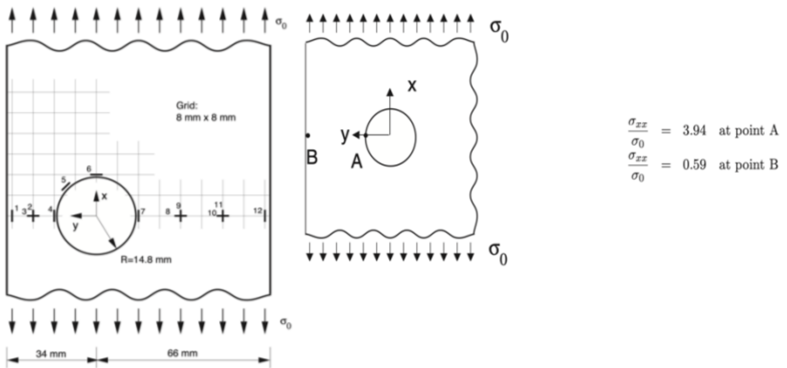

Mindlin’s derivation for $\sigma_{xx,point\ A}$ to a large degree agree with measured stress $\sigma_{xx,Gauge\ 4}$, with strain-gauge 4 registered stress values are about 20% smaller than the analytical solution. The possible cause for that might be that gauge 4 is not installed on the immediate edge of the hole, but to a small distance to the positive y-direction (with stress concentration decays away from the hole).
Strain-gauge 1 registered stress values are about 1.6 ~1.7 × $\sigma_{xx,point\ B}$, with possible reason be gauge 1 is not installed sufficiently far from the hole edge, with a distance of 16mm between gauge 1 and gauge 4 which is comparable to the hole distance of 14.8mm, a residual stress concentration still present at gauge 1location.

∘Symmetrically located hole, with the plate under 12kN (left), 16kN(right) uniaxial tension.

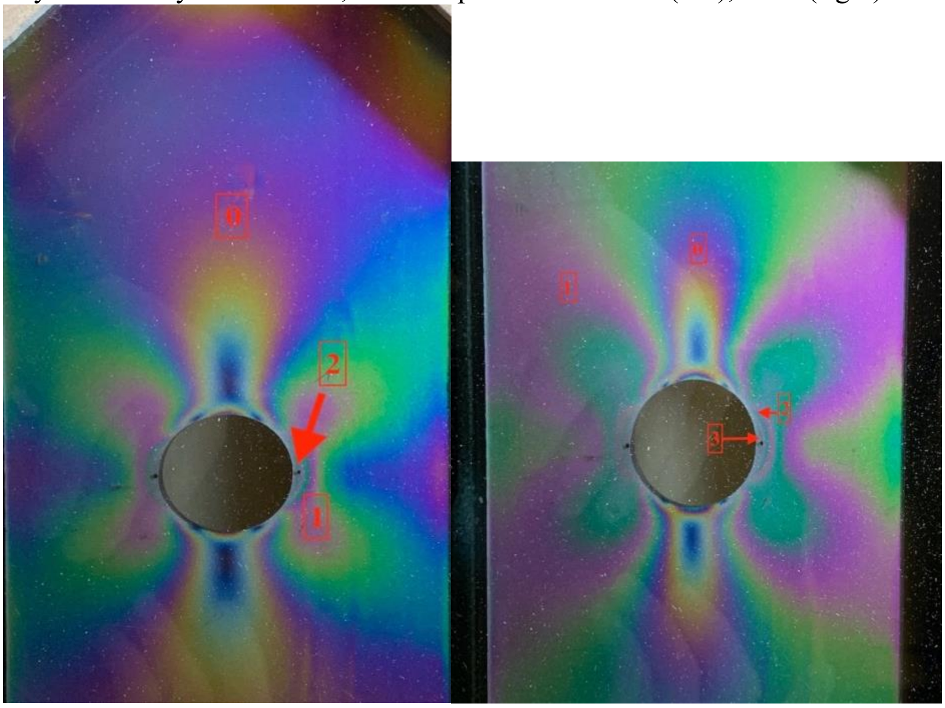

∘Asymmetrically located hole under unknown uniaxial tension (>4kN). (Moodle Image Repertoire for analysis: photoelasticity2)

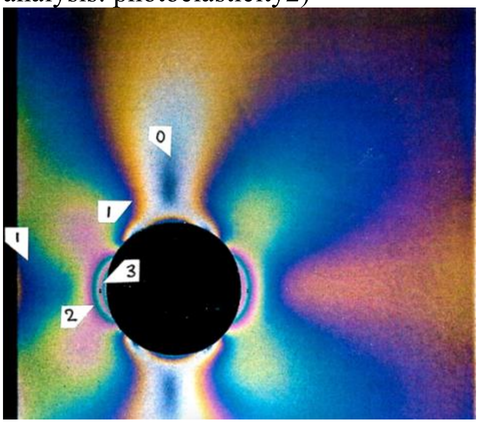

Marked fringes 0 join points in the plate with principal stress difference of 63.5 MPa, fringes 1 correspond with principal stress difference of 127MPa, fringes 2 ----190.5MPa, fringes 3----254MPa.

∘Instron: PIV/DIC analysis for symmetrically located hole.

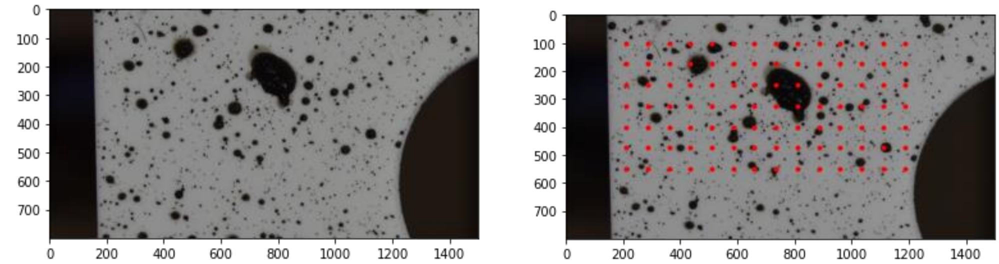

(Above) selected regular mesh grid of subsets (radius=50 pixels) for analysis.

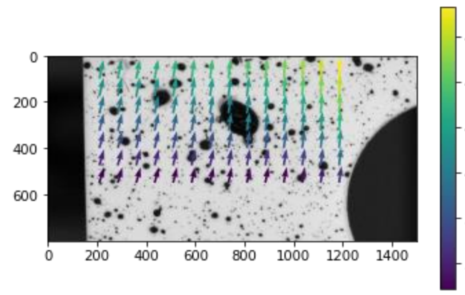

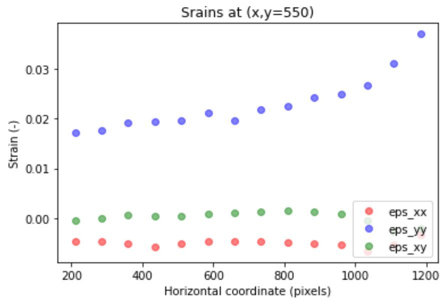

∘(Above)displacement field at selected meshgrid.

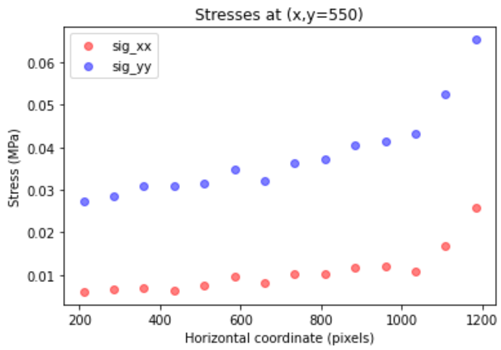

(In PIV/DIC analysis: x represents horizontal direction, y represents vertical direction)
It can be seen that:
1.At close proximities of the hole (x-direction 800----1200), σ_{xx} ,σ_{yy} and ε_{yy},grow significantly more than the remote stress.
2.The vertical extension movement ε_{yy} of the grid is much larger than the horizontal compressive movement $\varepsilon_{xx}$of the grid. With higher ε_{yy}closer to the hole. Shear strain $\varepsilon_{xy}$is negligible cross the whole field.

DISCUSSION

It is assumed in stress measurement calculations that at strain-gauge locations:
1,8 (on the symmetric plate); 1,4,7,12 (on the asymmetric plate) that gauges are located at the immediate edges of the thin plate/the hole, and therefore $\sigma_{yy} = 0$. (Stress must act within the plate, not the voids outside plate boundaries)
For the same reason, it is also assumed that at strain-gauge locations:
12 (on the symmetric plate); 5,6 (on the asymmetric plate)$\sigma_{yy} or\ \sigma_{xy} = 0$.
Due to the fact strain gauges are unlikely to be mounted directly on the edges of the plates, such assumption could cause discrepancies between measurements/calculations and analytical solutions.

For the plate with symmetrically located hole, it is shown in the strain-gauge measurements that both strain and stress distribution near the hole is non-linear regard to remote loading stress σ_0. With only small increase in measured stresses and strains (σ_{xx}, σ_{yy}, ε_{xx}, ε_{yy}), when loading doubled from 2kN to 4kN.
For the plate with asymmetrically located hole, it is shown in the strain-gauge measurements that both strain and stress distribution in the vicinity of the hole is possibly linear to the remote loading stress σ_0. When loading doubled from 2kN to 4kN, the recorded stress and strain values in general increased slightly more than 2 times

Photoelasticity method is only suitable when the plate is under high tensile loading, where high stress concentration is present in the vicinity of the hole. Since the requirement for each fringe to occur is a rather large difference in principal stresses. (63.5Mpa); under 2kN and 4kN of tensile loading condition where strain-gauges could give σ_{xx} and σ_{yy}measurement, the differences in principal stress were not large enough to produce the first fringe, which renders photoelasticity method unsuitable in such conditions.

The advantage of photoelasticity method is that it provides an overall view of the stress field distribution across the whole plate and can quickly visualise the changes in stress distributions as the remote tensile loading act on the plate changes.

The physical size of strain gauges meant that they cannot be placed at immediate edge of the plate, circumference of a hole or notch etc. It resulted in the inability to accurately measure the stress concentration at the boundaries of geometric discontinuities where the highest stress often distributed. And strain gauges can only give limited amount of point measurement, from which can be hard to intemperate the full picture of stress distribution.
The advantage of strain-gauge method is that it can provide numeric values of stress and strain at chosen locations, which is not possible through photoelasticity.

DIC/PIV can provide strain/stress data from more points than strain-gauge method, and the data is generated in graph format which make it easier to visualise the general trend in the stress/strain distribution.
However, not everywhere on the plane can be used as the targeted tracking surface and select subsets on it, whenever the displacement of speckles cannot be rendered by the program, such method cannot be functional. (might be solved if the software is not run on a webpage)
Subsets radius cannot be reduced infinitely, once their radius is smaller than the typical size of ink speckles, generated results start becoming unreliable.

CONCLUSION

The stress and strain distribution often highly concentrated around geometric discontinuities (in this lab, circular holes) in loaded components, which in practical term without reinforcement or proper placement, holes in a component can potentially initiate fracture, fatigue and crack. Such stress concentration should be properly calculated around any unavoidable holes in a structure, even it is magnitude decays away very quickly once getting sufficiently far (1.5 x radius) away from the holes.

ANNEX

	Symmetric Plate		
Gauge no	Vb	V0 (2kN)	V0 (4kN)
1	0.19	0.75	0.76
2	1.10	0.89	0.89
3	0.15	0.81	0.82
4	1.11	0.90	0.90
5	0.08	0.81	0.82
6	0.01	0.97	0.98
7	1.05	0.80	0.80
8	0.01	0.67	0.69
9	0.26	0.83	0.83
10	0.43	0.86	0.86
11	1.09	0.73	0.72
12	0.22	0.60	0.60

	Asymmetric Plate		
Gauge no	Vb	V0 (2kN)	V0 (4kN)
1	0.96	1.15	1.38
2	1.04	1.33	1.67
3	0.88	0.84	0.78
4	1.01	1.64	2.31
5	1.02	1.15	1.33
6	0.96	0.75	0.55
7	0.98	1.54	2.14
8	0.97	0.95	0.92
9	1.04	1.25	1.50
10	0.89	0.84	0.79
11	1.06	1.24	1.45
12	1.00	1.15	1.33

	Symmetric Plate			Asymmetric Plate	
Gauge No	$\varepsilon(2kN)$	$\varepsilon(4kN)$	*Gauge No*	$\varepsilon(2kN)$	$\varepsilon(4kN)$
1	0.000467	0.000475	1	0.000158	0.000350
2	-0.000175	-0.000175	2	0.000242	0.000525
3	0.000550	0.000559	3	-0.000033	-0.000083
4	-0.000175	-0.000175	4	0.000525	0.001085
5	0.000609	0.000617	5	0.000108	0.000258
6	0.000801	0.000809	6	-0.000175	-0.000342
7	-0.000208	-0.000208	7	0.000467	0.000968
8	0.000550	0.000567	8	-0.000017	-0.000042
9	0.000475	0.000475	9	0.000175	0.000383
10	0.000358	0.000358	10	-0.000042	-0.000083
11	-0.000300	-0.000308	11	0.000150	0.000325
12	0.000317	0.000317	12	0.000125	0.000275

Symmetric Plate (2kN)					
Gauge No	$\sigma_{xx}/10^7\,Pa$	*Gauge No*	$\sigma_{yy}/10^5 Pa$	*Gauge No*	$\sigma_{xy}/10^7$Pa
1	3.269	2	9.0338	10	-1.424
3	3.880	4	24.33		
5	4.343	7	42.68		
6	5.748	11	-112.5		
8	3.850	12	221.9		
9	2.954				

Asymmetric Plate (2kN)					
Gauge No	$\sigma_{xx}/10^7 Pa$	*Gauge No*	$\sigma_{yy}/10^6 Pa$	*Gauge No*	$\sigma_{xy}/10^6 Pa$
1	1.106	3	3.681	5	3.658
2	1.815	6	-11.900		
4	3.675	8	3.201		
7	3.269	10	0.589		
9	1.331				
11	1.069				
12	0.875				

Symmetric Plate (4kN)					
Gauge No	$\sigma_{xx}/10^7 Pa$	*Gauge No*	$\sigma_{yy}/10^5 Pa$	*Gauge No*	$\sigma_{xy}/10^7 Pa$
1	3.325	2	11.37	10	-1.45
3	3.951	4	26.402		
5	4.406	7	44.75		
6	5.811	11	-120.385		
8	3.969	12	221.9		
9	2.928				

Asymmetric Plate (4kN)					
Gauge No	$\sigma_{xx}/10^7 Pa$	*Gauge No*	$\sigma_{yy}/10^6 Pa$	*Gauge No*	$\sigma_{xy}/10^6 Pa$
1	2.450	3	7.090	5	6.026
2	3.909	6	-23.800		
4	7.595	8	6.629		
7	6.776	10	1.905		
9	2.900				
11	2.338				
12	1.925				